

Water as a Promoter and Catalyst for Dioxxygen Electrochemistry in Aqueous and Organic Media

Jakub Staszak-Jirkovský,^{†,¶} Ram Subbaraman,[†] Dusan Strmcnik,^{†,¶} Katharine L. Harrison,^{‡,¶} Charles E. Diesendruck,^{§,¶} Rajeev Assary,^{†,¶} Otakar Frank,^{||} Lukáš Kobr,[†] Gustav K. H. Wiberg,[†] Bostjan Genorio,^{†,#,¶} Justin G. Connell,^{†,¶} Pietro P. Lopes,^{†,¶} Vojislav R. Stamenkovic,^{†,¶} Larry Curtiss,^{†,¶} Jeffrey S. Moore,^{§,¶} Kevin R. Zavadil,^{‡,¶} and Nenad M. Markovic*,^{†,¶}

[†]Materials Science Division, Argonne National Laboratory, 9700 South Cass Avenue, Argonne, Illinois 60439, United States

[‡]Sandia National Laboratory, P.O. Box 5800, Albuquerque, New Mexico 87185, United States

[§]University of Illinois at Urbana–Champaign, Urbana, Illinois 61801, United States

^{||}Department of Electrochemical Materials, J. Heyrovsky Institute of Physical Chemistry, Prague, Czech Republic

[†]Northwestern University, Evanston, Illinois 60208, United States

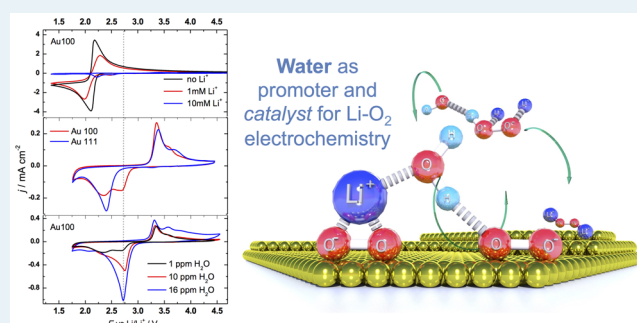
[#]Faculty of Chemistry and Chemical Technology, University of Ljubljana, Ljubljana, Slovenia

[¶]Joint Center for Energy Storage Research, Argonne National Laboratory, 9700 S Cass Avenue, Argonne, Illinois 60439, United States

Supporting Information

ABSTRACT: Water and oxygen electrochemistry lies at the heart of interfacial processes controlling energy transformations in fuel cells, electrolyzers, and batteries. Here, by comparing results for the ORR obtained in alkaline aqueous media to those obtained in ultradry organic electrolytes with known amounts of H_2O added intentionally, we propose a new rationale in which water itself plays an important role in determining the reaction kinetics. This effect derives from the formation of $\text{HO}_{\text{ad}}\cdots\text{H}_2\text{O}$ (aqueous solutions) and $\text{LiO}_2\cdots\text{H}_2\text{O}$ (organic solvents) complexes that place water in a configurationally favorable position for proton transfer to weakly adsorbed intermediates. We also find that, even at low concentrations (<10 ppm), water acts simultaneously as a promoter and as a catalyst in the production of Li_2O_2 , regenerating itself through a sequence of steps that include the formation and recombination of H^+ and OH^- . We conclude that, although the binding energy between metal surfaces and oxygen intermediates is an important descriptor in electrocatalysis, understanding the role of water as a proton-donor reactant may explain many anomalous features in electrocatalysis at metal–liquid interfaces.

KEYWORDS: *electrocatalysis, oxygen reduction reaction, lithium–oxygen, water networks, batteries, activated water*



1. INTRODUCTION

The diverse set of interactions mediated by water and oxygen have been the subject of broad-ranging study,^{1–6} and the complexities of these interactions are particularly important in understanding the phenomena governing chemical reactions at electrified solid–liquid interfaces. One property that sets aqueous electrochemical interfaces apart from all other interfaces is the potential-dependent interactions (van der Waals forces) of water molecules with species in the so-called “double layer”: i.e., interactions with neighboring ions located in the outer Helmholtz plane (OHP) and with covalently bonded spectator/intermediate species located in the inner Helmholtz plane (IHP).^{7,8} The nature and strength of these interactions completely control the structure of the double layer and rely on an interplay between the physicochemical

properties of water molecules themselves (dipole moment and hydrogen bonding), the nature of the supporting electrolyte (solvation effects), and the nature of the electrode material used (covalent bonding of adsorbates). In addition to such structural effects, water-controlled interactions in the double layer also play a decisive role in electrocatalytic processes where either water molecules or adsorbed water dissociation products (commonly denoted as OH_{ad} and H_{ad}) actively participate in the reaction pathway. Two particularly well-studied examples involving water as a reactant are the hydrogen evolution reaction (HER; 2H₂O + 2e⁻ = H₂ +

Received: August 13, 2015

Revised: September 23, 2015

Published: September 30, 2015



2OH^-) in alkaline electrolyzers^{9–11} and the oxygen reduction reaction (ORR; $\text{O}_2 + 2\text{H}_2\text{O} + 4\text{e}^- = 4\text{OH}$) in alkaline fuel cells.¹² For the ORR, it is generally assumed that the reaction kinetics for both acid and alkaline media are mainly governed by the binding energies between the catalyst and oxygenated intermediates (O_2^- , HO_2^- , OH^-), with only limited spectroscopic evidence confirming the presence of these species at the interface.^{13–17} In particular, for surfaces with weak oxygen binding energies (e.g., Au), the ORR rate is limited by the activation of O_2 , and for surfaces with oxygen binding energies that are too strong (e.g., Ru and Ir),^{18,19} the rate is limited by the removal of hydroxyl groups from the catalyst surface. The optimal oxygen binding energy and, thus, the highest activity in acidic solutions in the existing volcano relationships (plots which generally express the rate of an electrocatalytic reaction as a function of more fundamental properties of the catalyst, known as descriptors) is found to be the so-called Pt(111)-skin structure, which is formed after the annealing of a Pt₃Ni(111) single crystal.²⁰

Much less attention has been placed on understanding the “ORR volcano landscape” in alkaline solutions, where Au(100) is found to be one of the most active catalysts—it is even more active than Pt(111).^{21–23} This paradoxical behavior of Au(100) suggests that, in addition to oxygen binding energy, the reactivity of water molecules might also contribute to the anomalous kinetics of the ORR, as water is the only proton-donor reactant in these environments. However, simultaneously probing the interfacial reactivity of water and oxygen intermediates in aqueous environments is an incredibly challenging task, even on well-characterized single-crystal surfaces.

In many respects the subject of dioxygen surface electrochemistry in organic solvents is much less advanced than the corresponding understanding of interfaces in aqueous systems.^{23,24} This is due to the longstanding difficulty associated with developing *in situ* methods that are capable of characterizing interfaces at atomic/molecular levels in organic solvents. One prime example is Li–O₂ electrochemistry, which has primarily been studied on ill-defined, polycrystalline, and/or high-surface-area cathode materials in organic solvents containing trace levels of water and other impurities that, even in ppm levels, can dominate interfacial properties in organic environments.^{25–30} Not surprisingly, then, it has been very difficult to reproduce many claims of high rechargeability and reversibility of the Li–O₂ battery systems. This intrinsic disparity in understanding water-based and organic-based solvents, however, has a tendency to mask the inherently close ties that may exist between interfacial phenomena in aqueous and organic environments, especially regarding the electrochemical reduction of dioxygen.

Here, we build a bridge between dioxygen electrochemistry in alkaline- and ether-based environments in order to yield unique insights into the synergistic nature of double-layer interactions and provide an integrated, stepwise link between inherently multicomponent electrochemical interfaces and the role of water in controlling the kinetics of the ORR in aqueous media. Using these insights, we were also able to assess the impact of water on Li–O₂ electrochemistry in organic solvents. One key finding was that, by controlling the water content in organic solvents, dioxygen electrochemistry on Au(111) and Au(100) becomes structure sensitive only in the presence of ppm levels of water. This knowledge was then transferred to alkaline electrolytes, for which we propose that the exceptional

activity of the ORR on Au(100) arises due to the interaction between OH_{ad} and water molecules, which form an activated water complex (HO_{ad}···H₂O) that places water in a configurationally favorable position for proton transfer to weakly adsorbed O₂⁻/HO₂⁻ intermediates. The optimal balance between the availability of metal sites for the formation of oxygen intermediates and the availability of surface water molecules is observed on Pt₃Ni(111), which exhibits the highest activity ever measured for the ORR. The knowledge from alkaline solutions is then transferred back to ether-based environments to find that, even at low concentrations (<10 ppm), water acts simultaneously as a promoter and as a *catalyst* in the production of Li₂O₂, regenerating itself through a sequence of steps that include the formation and recombination of H⁺ and OH⁻. We conclude that although the binding energy between metal surfaces and oxygen intermediates is an important descriptor in electrocatalysis, understanding the role of water as a proton-donor reactant may explain many anomalous features in electrocatalysis at metal–liquid interfaces.

2. RESULTS AND DISCUSSION

2.1. Structure–Function Relationships for Dioxygen Electrochemistry in Organic Media.

One key aspect of dioxygen electrochemistry on polycrystalline electrode materials in aprotic solvents is that O₂ is reduced by a reversible one-electron process to a relatively stable superoxide ion (O₂ + e⁻ ⇌ O₂⁻).^{24,31–33} Sawyer and co-workers in particular pioneered these studies, exploring how the peak potential for the dioxygen reduction process (i.e., reversibility) depends on the extent of superoxide ion solvation (effects of media) and the nature of electrode materials (Pt, Au, Hg).^{24,34} They found that the reduction potential for the O₂/O₂⁻ couple shifts to more positive values as the solvation properties of the media increase, which is consistent with the effect of the solvation energy for O₂⁻ on the reversible potential (especially in the presence of water with its unique heat of hydration). The authors also proposed that there is a weak interaction between metal surfaces and either superoxide ions or their disproportionation products, signaling that the superoxide formation might be an inner-sphere reaction. Inner-sphere reactions involve direct bond formation and orbital overlap with the surface, prime examples of which are the structure-sensitive adsorption of hydroxyl species from the bulk of electrolytes and the kinetics of the ORR on metal surfaces in aqueous media.^{35,36} In contrast, outer-sphere reactions are independent of the nature of electrode materials or the geometry of surface atoms so that they involve weak van der Waals forces among solvated ions, covalently bonded adsorbates, and “free water molecules”.^{7–9,37} Surprisingly, it is still unknown whether the O₂ + e⁻ = O₂⁻ reaction is an inner-sphere or outer-sphere process—at least there is no clear-cut evidence from experimental studies. To resolve this issue, we examine the reduction of O₂ to O₂⁻ on Au(100) and Au(111) surfaces in a clean, water-free 1,2-dimethoxyethane (DME) solvent with TBAPF₆ as the salt. We chose to study this system for two key reasons: (i) surface structures of Au single-crystal surfaces are well-defined, providing direct insight into structure–function relationships and (ii) by systematic addition of water to a dry solvent, it may also be possible to gain insight into the role of water in the electrochemical reduction of dioxygen in aqueous-based environments.

Figure 1a illustrates cyclic voltammograms (CVs) for the reduction of dioxygen (1 atm) on Au(100) and Au(111) in

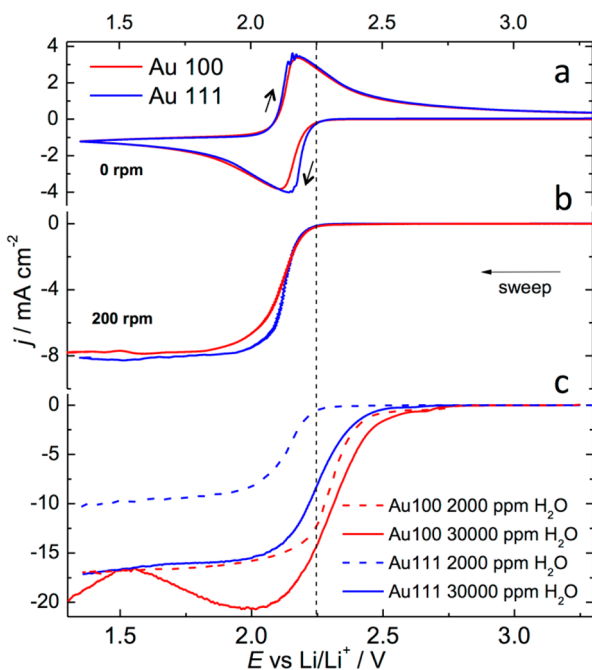


Figure 1. Effect of water on superoxo electrochemistry on Au(*hkl*) in ether-based electrolytes: (a) cyclic voltammetry (CV) on Au(*hkl*) in dry DME and 0.3 M TBAPF₆ (<1 ppm of H₂O) saturated with O₂; (b) rotating-disk-electrode (RDE) experiment in the same electrolyte (rotation rate 200 rpm); (c) RDE results on Au(100) and Au(111) in the same electrolyte containing 2000 and 30000 ppm of water (rotation rate 200 rpm; sweep rate 100 mV s⁻¹).

DME. Significantly, a reversible O₂/O₂⁻ redox couple centered at ~ 2.2 V is observed on both surfaces, suggesting that the superoxide electrochemistry is *not* a structure-sensitive process; e.g., the O₂ + e⁻ = O₂⁻ reaction is an outer-sphere electron transfer process. The fact that the polarization curves summarized in Figure 1b are essentially identical on both Au single crystals further confirms that the O₂⁻ formation is indeed an outer-sphere electron transfer process (see also Figure S1 in the Supporting Information). Significantly, the ORR rapidly becomes a structure-sensitive process in the presence of >2000 ppm of water (Figure 1c). The observed difference in activity between the two surfaces is identical with that observed in alkaline environments: the Au(100) surface is far more active than the Au(111) surface. Keeping in mind that the heat of hydration for gaseous O₂⁻ (418 kJ) is insensitive to surface structure, the observed structural differences in the onset potential and current densities for the ORR on Au(111) and Au(100) cannot be explained solely on the basis of the effect of heat of hydration on the reversible potential for the O₂/O₂⁻ redox couple as discussed by Sawyer and co-workers.^{24,34} Given that water is a proton donor controlling the formation of HO₂⁻ and/or OH reaction intermediates, it is reasonable to anticipate that the structure–function relationships for the ORR on Au(*hkl*) might be governed by the structure-sensitive role of water. We conclude, therefore, that the structure sensitivity observed for the ORR in Figure 1c arises primarily due to the water-controlled formation of protonated intermediates. As we discuss further below, we will use a similar argument to explain the unique activity of Au(100) in alkaline solutions. For clarity,

we will first focus on results for Au single crystals in alkaline solutions and will return to results on other surfaces at the end of the paper.

2.2. Dioxygen Electrochemistry in Aqueous Media.

Recall that in alkaline solutions Au(100) exhibits an unusually high activity (4e⁻ reduction) that is as puzzling today as it was three decades ago, when it was realized that there are intriguing relationships between ORR reactivity and the surface coverage of OH_{ad} formed in O₂-free electrolytes (OH⁻ = OH_{ad} + e⁻).³⁸ Consistent with earlier reports,^{21–23,39} Figure 2a shows that a wide “double layer” region is formed in O₂-free electrolytes, followed by the structure-sensitive, reversible formation of OH_{ad} between 0.65 and 1.15 V. The adsorption of OH⁻ on metal surfaces involves covalent bonding, and the surface coverage by OH_{ad} (Θ_{OHad}) is strongly dependent on both the nature of electrode materials as well as the structure of surface atoms. Inspection of Figure 2a reveals that Θ_{OHad} is always higher on Au(100) (~ 0.25 ML) than on Au(111) (~ 0.15 ML), which is in agreement with previous results.^{21–23,39} In general, it has been proposed that OH_{ad} is merely a spectator to the ORR, poisoning metal sites needed for the adsorption of O₂ and reaction intermediates.^{4,20} In the case of gold, however, Figure 2b shows the opposite trend—Au (100) displays much higher activity for the ORR, and the transition from the 4e⁻ to 2e⁻ reduction pathway at ~ 0.6 V coincides with the desorption of OH_{ad}—suggesting that OH_{ad} is, in fact, a promoter. In light of the results discussed above for organic systems with various levels of H₂O added intentionally, it is now possible to rationalize the perplexing role of OH_{ad} in alkaline solutions.

Here we propose that an alternative, yet related, facet of the ORR in alkaline media may involve the “activation” of water by OH_{ad} so that protonation of oxygen intermediates becomes facile. As schematically depicted in Figure 2c, this process may occur through the formation of hydrogen-bonded complexes between covalently bonded OH_{ad} and water molecules (e.g., HO_{ad}···H-OH). The degree of coverage by these complexes on the surface (Θ_{complex}) is proportional to Θ_{OHad} and may in fact be the same. The activated complex schematic is based on our previous findings that OH_{ad} can interact with hydrated cations in the double layer, leading to the formation of HO_{ad}···K⁺ + (H-OH)_x clusters that affect the reactivity of electrochemical interfaces.⁷ Returning to the HO_{ad}···H-OH interaction, Figure 2d shows that, even on a positively charged surface, as in the case of the ORR above 0.7 V, the interaction of OH_{ad} with water molecules can place water in a configurationally favorable position for proton transfer to O₂⁻ and HO₂⁻ intermediates: e.g., with hydrogen pointing down to the surface so that it can react easily with intermediates that are formed on adjacent metal sites. This proton transfer can take place in two discrete steps: (i) first from one HO_{ad}···H-OH complex to adsorbed O₂⁻ species, leading to formation of HO₂⁻ (see schematics in Figure 2d), and (ii) if there is a critical Θ_{complex} (e.g., adjacent HO_{ad}···H-OH complex), additional proton transfer occurring to the newly formed HO₂⁻ species on the neighboring gold atoms so that the reaction leads to the formation of OH⁻ species. As depicted in Figure 2e, the second step is governed by the colocation of two HO_{ad}···H-OH complexes, along with bare metal sites for stabilizing the HO₂⁻ species. Overall, then, the activity of Au(*hkl*) is determined by both the degree of coverage by these complexes on the surface (Θ_{complex}) and the presence of bare gold sites for the formation of reaction intermediates. For example, if Θ_{complex} is low, there are a sufficient number of metal sites for the formation of OH₂⁻

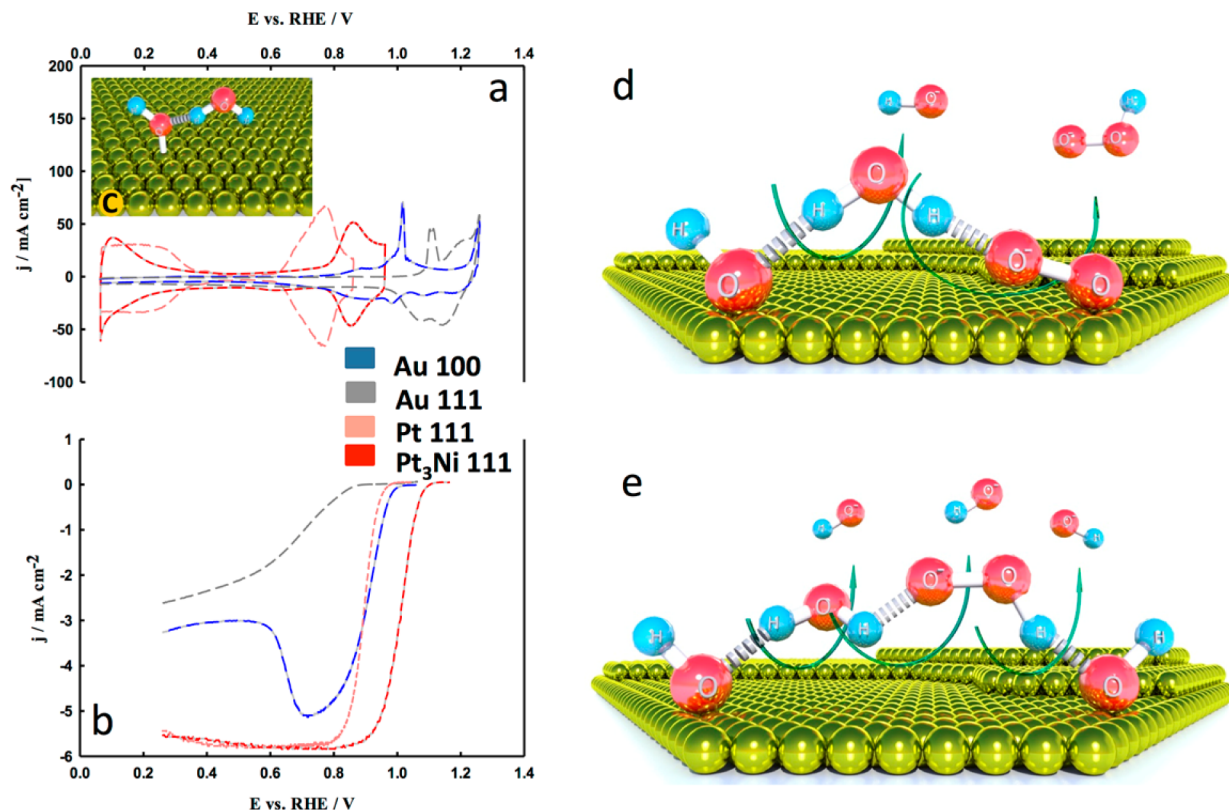


Figure 2. ORR on metal surfaces in alkaline environments, with water as a promoter: (a) CVs of Au(111), Au(100), Pt(111), and Pt₃Ni(111) in 0.1 M KOH; (b) polarization curves for the ORR in the same solution, showing that the activity increases in the order Pt₃Ni(111) >> Au(100) > Pt(111) > Au(111), with Pt₃Ni(111) being the most active catalyst for the ORR ever observed in aqueous environments; (c) schematic of a proposed OH_{ad}-H₂O complex (“activated water”) formed via hydrogen bonding, emphasizing that this complex might be a key descriptor for controlling the reaction pathway of the ORR in aqueous environments; (d) schematic representation of the effect of “activated water” on peroxide and hydroxyl formation on surfaces with a low coverage of OH_{ad}-H₂O complexes; (e) schematic representation of further peroxide reduction on a surface covered with two active OH_{ad} centers that are required for the peroxide O–O bond cleavage and final production of three hydroxyl ions. Note that the schematics are meant to illustrate the most probable reaction pathway for the ORR on the basis of the results presented.

intermediates, but not enough adjacent sites also containing activated water for the reaction to proceed further. As a consequence, the ORR proceeds as a 2e⁻ process, as is the case for Au(111) in the entire potential region and for Au(100) below 0.7 V (Figure 2d). At intermediate values of Θ_{complex} the right ensemble of OH_{ad}···H₂O complexes and bare surface metal sites is present, enabling effective stabilization of the HO₂⁻ intermediate and further reduction to OH⁻ via a 4e⁻ pathway. This occurs via the presence of two OH_{ad} anchoring points for hydrogen bonding: one for the stabilization of HO₂⁻, and the second to activate water for a second proton transfer and the formation of 2OH⁻ species (Figure 2e). This is indeed the case for Au(100) between 0.9 and 0.7 V, where sufficient Θ_{complex} enables 4e⁻ reduction to occur. To further explore the importance of the activation of water in surface electrochemistry, we demonstrate in the following that other oxygenated species may also serve as an anchor to stabilize and activate water molecules at electrochemical interfaces, which we examine for the specific case of Li⁺-containing organic electrolytes.

2.3. Water’s Role in Aprotic Lithium Oxygen Electrochemistry: Promoter and Catalyst. We begin by examining the current–potential response to systematic Li⁺ addition in DME/TBAPF₆ under conditions identical with those utilized to study aprotic, lithium-free superoxide electrochemistry in Figure 1. Figure 3a illustrates the effect of Li⁺ concentration

on the rechargeability of Au(100), and a very similar response is also observed for Au(111) (Figure S2 in the Supporting Information). In the presence of 1 mM Li⁺, the most prominent features observed are the decrease of the O₂⁻/O₂ reversible peak intensity and the appearance of a small, yet clearly discernible, reduction current between 2.5 and 2.2 V. These features suggest that irreversible changes in dioxygen electrochemistry take place in the presence of Li⁺. The degree of irreversibility increases with the concentration of Li⁺, as shown in Figure 3a for Li⁺ concentrations up to 10 mM, and finally for a concentration of 0.3 M Li⁺ in Figure 3b. Regardless of the Li⁺ concentration, two points are important: (i) in a “dry” electrolyte, Au(100) is more active than Au(111) and (ii) the kinetics of the charging process (OER) are almost independent of the arrangement of gold surface atoms and are characterized by a sharp oxidation peak at 3.25 V and smaller, broader peak at more positive potentials. Considering that the formation of superoxide ions is reversible, but not structure-sensitive, in aprotic, lithium-free environments (Figure 1a), it is important to understand why the formation of Li–oxygen intermediates exhibits irreversibility and structure sensitivity in the presence of Li⁺.

To address this question, experiments were carried out in both dry electrolyte (≤ 1 ppm water) and electrolyte with small amounts of water added intentionally (in Figure 3c up to 16 ppm). Interestingly, during the discharge process a dramatic

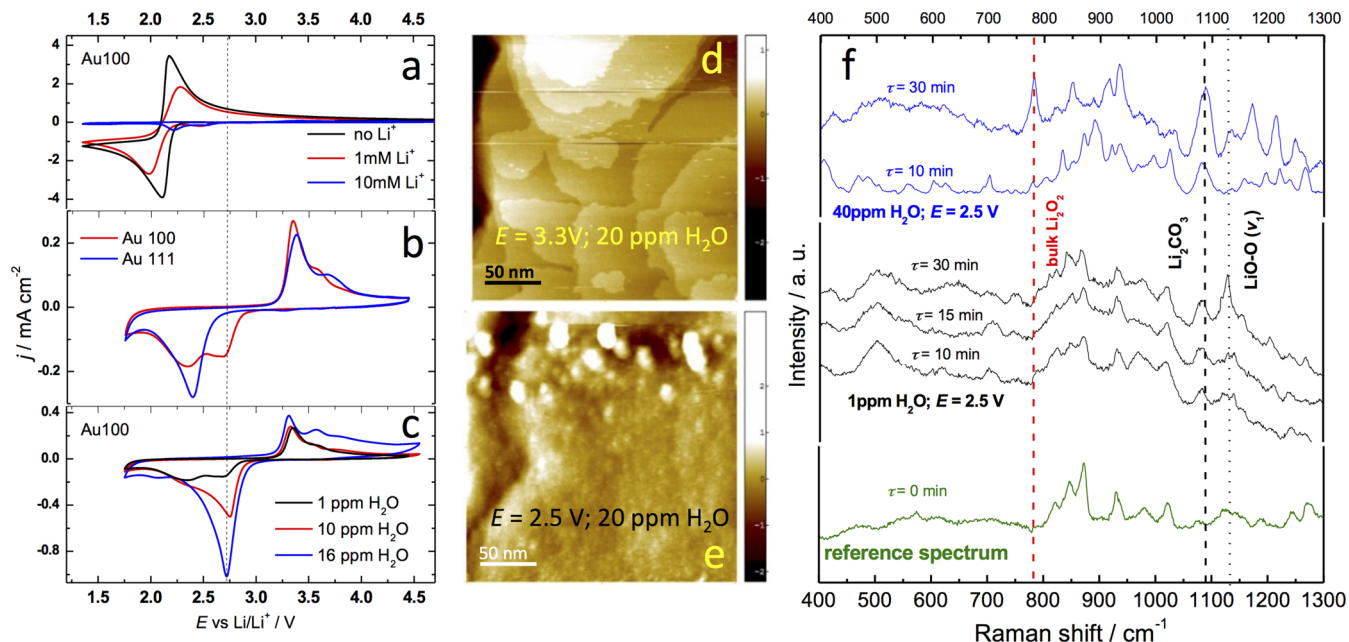


Figure 3. Water effect on oxygen electrochemistry in a presence of Li⁺, with water as a promotor and catalyst: (a) CV of Au(100) in dry DME and 0.3 M TBAPF₆ saturated with O₂ and various concentrations of Li⁺; (b) CV in O₂-saturated 0.1 M Li triflate for Au(100) and Au(111); (c) effect of various amounts of water on Li—O₂ electrochemistry on Au(100) (sweep rate 100 mV s⁻¹); (d) in situ AFM imaging of Au(111) in TEGDME/LiClO₄ saturated with O₂ at 3.5 V; (e) sample as in (d) held at 2.5 V for 30 min; (f) in situ Raman spectroscopy of a roughened gold electrode at 2.5 V in “dry” (1 ppm of H₂O) and “wet” (40 ppm of H₂O) electrolyte (DME, 0.1 M LiClO₄). The vertical lines are added to guide the eye. See also Figure S4 and text in the Supporting Information for additional details on Raman band assignment.

increase in charge is observed in the presence of only 10–16 ppm of H₂O on Au(100). Given that the addition of water has a negligible effect on the CV of Au(111) under the same experimental conditions (Figure S2B in the Supporting Information), the fact that structure sensitivity is observed for “dry” electrolytes in Figure 3b suggests that the presence of even 1 ppm of water (as verified by Karl Fischer titration) is enough to enhance the kinetics of the ORR and thus the formation of Li_x—O_y products on Au(100) surfaces in organic electrolytes. The morphology of the deposit was characterized with in situ atomic force microscopy (AFM), as shown for the Au(111) surface in Figure 3d,e (see also Figure S3 in the Supporting Information). While Figure 3d shows the characteristic topology of well-defined Au(111) terraces at an open circuit potential (3.3 V), Figure 3e shows that at 2.5 V (discharge) a film of unknown chemical identity forms rapidly ($\tau \approx 130$ s), which is comprised of clusters of nanoparticles that form a 2 nm thick film coating the Au surface (see also Figure S3 in the Supporting Information).

To chemically characterize the deposits formed during the ORR, we employed in situ Raman spectroscopy in the same environment used above. Time-dependent spectra were acquired during discharge at 2.5 V in an O₂-saturated solution for “dry” electrolytes and electrolytes with varying concentrations of water, summarized in Figure 3f. With 1 ppm of water present in the electrolyte, a band appears at ~ 1130 cm⁻¹ after 15 min and increases in intensity at 30 min. This vibrational frequency is assigned to the O—O stretch of bulk LiO₂^{40,41} and is the result of LiO₂ formation. In electrolyte with 40 ppm of water added, a sharp Li₂O₂ vibration at 785 cm⁻¹ clearly appears in the spectrum. The intensity of this peak increases with time, indicating that Li₂O₂ formation is significantly catalyzed in the presence of 40 ppm of water. An additional sharp, time-dependent peak at 1080 cm⁻¹ is also observed in 40

ppm of water, which likely corresponds to the formation of Li₂CO₃ resulting from the decomposition of DME^{28,42} (see also Figure S4 and Table S1 in the Supporting Information).

The key conclusion from the results in Figure 3 is that, while LiO₂ is the main product in dry electrolytes, the formation of Li₂O₂ is promoted in solutions with 15–40 ppm of water. It is surprising that such a small amount of water is not consumed, even after the prolonged discharge reaction time. One possible reason is summarized in Figure 4, where we identify five significant reaction steps that explain the role of water in Li—O₂ electrochemistry in organic solvents. This reaction scheme is also supported by computational results (Table S2 in the Supporting Information). The first step (step 1 → 2 in Figure 4b) involves electron transfer to dioxygen and reaction with Li⁺ to form LiO₂. This process occurs on gold surfaces both in the dry electrolyte and with small amounts of water being present, as evidenced by Raman peaks at ~ 1130 cm⁻¹ for both conditions in Figure 3f. In the second step (step 2 → 3), LiO₂ and water hydrogen bond to form activated water on the surface—the LiO₂···H₂O complex. In contrast to alkaline solutions and DME/TBAPF₆ solvents, the surface coverage of LiO₂ (Θ_{LiO_2}) is independent of the absolute concentration of water so that only a few ppm of water is sufficient to trigger the formation of LiO₂···H₂O complexes. We note that water molecules are preferentially located in the double layer due to their high polarizability, even in a huge excess of organic solvent. As in aqueous environments, step 3 → 4 involves the simultaneous reaction of water with O₂ and electron transfer, resulting in the partial dissociation of H₂O. Step 4 → 5 involves a second electron transfer to the resulting HO₂ radical to produce HO₂[−] and OH[−] anions. In step 5 → 6, HO₂[−] anions react with Li⁺ to form Li₂O₂ and a proton (2Li⁺ + HO₂[−] = Li₂O₂ + H⁺), which is captured experimentally by the time-increasing Li₂O₂ peak in the Raman spectra (Figure 3f) when

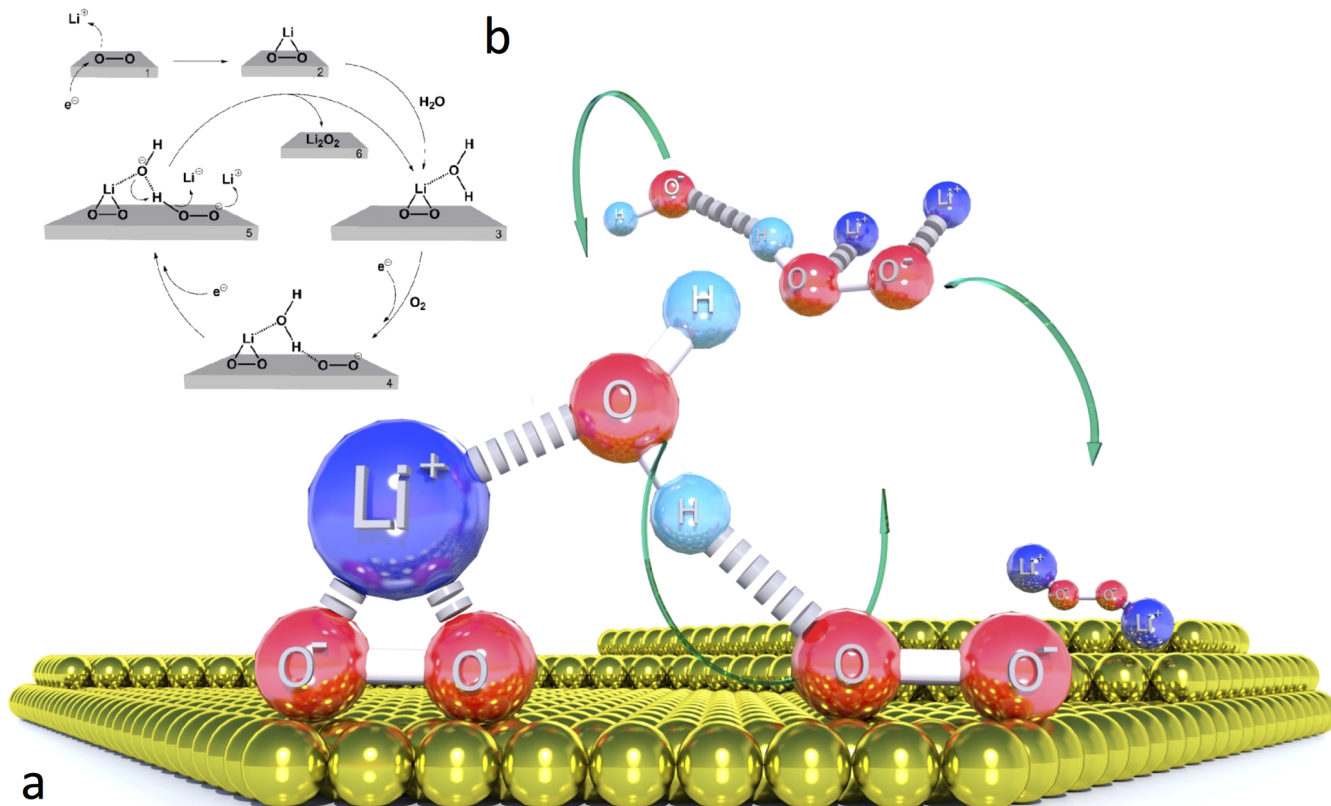


Figure 4. Water as catalyst and promoter in $\text{Li}-\text{O}_2$ electrochemistry. (a) Schematic illustration of bond formation/breaking events (denoted by arrows and dashed bond lines) associated with the “activated water” $\text{LiO}_2-\text{H}_2\text{O}$ complex, resulting in the protonation of O_2^- and formation of Li_2O_2 deposits in ether-based electrolytes. (b) Reaction scheme showing the “water cycle” initiated by the formation of LiO_2 and resulting in the catalyzed formation of Li_2O_2 . The scheme involves five main reactions: (i) LiO_2 formation (step 1-2); (ii) formation of the $\text{LiO}_2 \cdots \text{OH}_2$ complex through dipole–dipole interactions (step 2-3) (iii) interaction of the $\text{LiO}_2 \cdots \text{OH}_2$ complex with superoxide (step 3-4); (iv) proton and electron transfer to the superoxide molecule to form hydrogen peroxide (step 4-5) and finally (v) formation of Li_2O_2 (step 5-6) and regeneration of water (step 5-3). The slabs are added to illustrate that the processes are taking place at an electrode surface acting simultaneously as proton donor. The direction of the arrows follow the flow of electrons.

40 ppm of water is present. Crucially, the remaining OH^- can react with H^+ to regenerate the water molecule ($\text{OH}^- + \text{H}^+ = \text{H}_2\text{O}$), so that only a small amount of water is required to initiate a new catalytic cycle. The fact that such a small amount of water is not consumed during the reaction is strong evidence for the role of water as a *catalyst*, as well as a promoter, for $\text{Li}-\text{O}_2$ electrochemistry in organic solvents. Water acting as a catalyst has not, to the best of our knowledge, previously been reported for any electrochemical reaction.

3. CONCLUDING REMARKS

In this study we show that, by controlling the water content in organic solvents, dioxygen electrochemistry on $\text{Au}(111)$ and $\text{Au}(100)$ becomes structure sensitive only in the presence of water. Using this knowledge, we propose that the exceptional activity of the ORR on $\text{Au}(100)$ in alkaline electrolytes arises due to a similarly structure sensitive interaction between OH_{ad} species and water molecules, which forms hydrogen-bonded complexes ($\text{HO}_{\text{ad}} \cdots \text{H}_2\text{O}$) that place water in a configurationally favorable position for proton transfer to weakly adsorbed $\text{O}_2^-/\text{HO}_2^-$ intermediates. Therefore, we suggest that OH_{ad} may play a dual role on metal surfaces; e.g., it provides sites for the formation of $\text{HO}_{\text{ad}} \cdots \text{H}-\text{OH}$ complexes (acting as a promotor

and blocks sites for adsorption of O_2 , O_2^- , and HO_2^- (acting as a spectator). The promoting role of these complexes is summarized schematically in Figure 2d,e. The balance between these two opposing effects determines the catalytic activity. This hypothesis is further supported if we expand our analysis to other single-crystal surfaces in alkaline solution. Specifically, on comparison of surface coverage by OH_{ad} (Θ_{complex} ; see Experimental Methods for details on OH_{ad} estimation) on $\text{Pt}(111)$ (~ 0.55 ML) and $\text{Au}(100)$ (~ 0.25 ML) in Figure 2a with ORR activity in Figure 2b, it is clear that Θ_{complex} on $\text{Pt}(111)$ is higher than that on $\text{Au}(100)$, but with a lower reaction rate, suggesting that Θ_{complex} is too high. The fundamental question is as follows: what is the optimal Θ_{complex} value? We attempted to answer this question using the so-called $\text{Pt}(111)$ -skin structure formed on $\text{Pt}_3\text{Ni}(111)$ single crystals after temperature-induced segregation, which was chosen due to the fact that it is the best catalyst for the ORR in acidic media.²⁰ As shown in Figure 2, Θ_{complex} on the $\text{Pt}(111)$ -skin surface (~ 0.4 ML) is lower than that on $\text{Pt}(111)$ but higher than that on $\text{Au}(100)$, signaling that this surface may have an optimal balance of active sites. Indeed, Figure 2b reveals that the $\text{Pt}(111)$ -skin is more active than $\text{Au}(100)$; in fact, the observed activity is the highest ever measured in electrocatalysis of the ORR.

Furthermore, the proposed role of activated water was also used to explain the Li–O₂ electrochemistry in organic solvents: namely, LiO₂ serves as a promotor to activate water so that, even at low concentrations (<10 ppm), water acts simultaneously as a promoter and as a *catalyst* in the production of Li₂O₂, regenerating itself through a sequence of steps that include the formation and recombination of H⁺ and OH⁻. We note in passing that this knowledge can be used to explain the perplexing promoting role of the so-called underpotential-deposited (UPD) metals^{17,43,44} such as Pb, Bi, and Tl on the ORR in aqueous-based solutions. For example, a polycrystalline gold electrode partially covered by UPD adatoms (~0.3 ML) exhibits 4e⁻ reduction, in comparison with the 2e⁻ reduction observed under identical conditions on bare Au surfaces. Given that these metals are generally deposited in an oxygenated form, e.g., as hydroxyl oxides (resembling deposited LiO₂), we propose that UPD metals influence the ORR via a similar promoting effect, providing enough metal sites for the electron transfer and two anchoring points for hydrogen bond formation among water, peroxide, and oxygenated species (see schematics in Figure 2d,e). As in the case of Li–O₂ systems, too high of a coverage by UPD adatoms ($\Theta > 0.4$ ML) leads to a sharp deactivation of the ORR, as they block the necessary bare metal sites, as LiO₂ and Li₂O₂ do in the Li–O₂ systems discussed above. These results, taken together, suggest that if we are able to better understand the role of water at electrochemical interfaces then it will be possible further to rationalize, and ultimately understand, electrocatalysis in both aqueous and organic environments.

4. EXPERIMENTAL METHODS

4.1. Chemicals. The aqueous experiments were carried out in Milli-Q water and KOH (Aldrich) 99.995% trace metal basis. The DME used in the nonaqueous experiments was purchased from BASF and was subject to complex additional purification consisting of chemical, distillation, and adsorption methods. TBAPF₆, LiClO₄, and ⁶LiClO₄ were purchased from Aldrich (electrochemical grade), and LiTFS (Li triflate) was obtained from BASF. TEGDME was purchased from Aldrich and was double-distilled from Na. The salts were dried in a vacuum oven at 180 °C.

4.2. Electrochemistry. Au(100) and Au(111) crystals of 6 mm diameter were used in the experiments. Au crystals were annealed before each experiment using RF induction heating at 800 °C under a H₂ (3%)/Ar stream. The water content in electrolytes was measured by Karl Fischer titration (Mettler-Toledo) placed inside an Ar-filled glovebox with the moisture level below 0.5 ppm. The water content of the “dry” electrolytes was measured to be <1 ppm (after mixing the solvent with salt). All experiments were carried out inside an Ar-filled glovebox and in a homemade glass cell with a total volume of electrolyte solution of about ~20 mL in a typical experiment. The cell was sealed with a Kel-F lid equipped with FEP Swagelok fittings to provide contact inside the cell as well as a gas inlet and outlet. A three-electrode system was employed with gold wire as the counter and Ag/AgNO₃ as the reference electrode. The counter and reference electrodes were kept in separate compartments, and the Ag/AgNO₃ reference was divided from the rest of the cell by a Vycor frit. The working electrode was tightly held in a PCTFE collet and sealed by PTFE on the sides to ensure that only the defined surface was in contact with the electrolyte. The reference potential was calibrated by measurement of the

ferrocene redox couple. For experiments in organic solvents, all potentials were recalculated vs the standard Li/Li⁺ couple. Aqueous experiments were performed in a PTFE cell in a three-electrode configuration. An Ag/AgCl reference electrode was employed, and the potential was recalculated with respect to the reversible hydrogen electrode (RHE) scale. A Pine Instruments rotator was used in the RDE measurements, and Autolab potentiostats were used to perform the electrochemical measurements. *iR* drop correction was used in all the experiments. Calculation of OH_{ad} coverage in aqueous environments was done by integrating the voltammetry up to 1 V vs RHE, and an average from both anodic and cathodic scans was used in the values shown.

4.3. Raman. A Renishaw inVia Raman spectrometer was used in these experiments, and the *in situ* experiments were carried out using Leica inverted Raman microscope optics. A homemade sealed spectroscopic cell equipped with a quartz optical window was employed. A 785 nm laser was used for the excitation, and a 50× magnification, long working distance objective from Olympus was used throughout the measurements. The roughened gold electrode was prepared as reported elsewhere.¹⁷

4.4. AFM. Electrochemical AFM measurements were performed using an Agilent 5500 microscope housed in a glovebox supplied by a continuous flow of ultrahigh-purity Ar (<1 ppm of H₂O). Moisture levels were measured (Kahn) to be less than 20 ppm during the course of an experiment. Au(111) textured films on mica (Agilent) were flame annealed (butane) immediately prior to loading into the glovebox and assembly of the electrochemical cell. Li and Au were used as reference and counter electrodes, respectively. Low force AFM measurements were made in contact mode using a 240 mN m⁻¹ trigonal cantilever (Bruker, SNL) at minimum deflection.

4.5. Computational Details. All calculations presented herein were computed using the Gaussian 09 software. The B3LYP/6-31+G(d) level of theory was used to compute electronic energies, enthalpies, and spectra, unless mentioned otherwise.⁴⁵ This level of theory provides adequate accuracy for computing reaction energetics and for simulating vibrational and Raman spectra of various organic molecules and lithium–oxygen complexes. Selected reaction energies were computed using the accurate G4MP2 level of theory.

■ ASSOCIATED CONTENT

S Supporting Information

The Supporting Information is available free of charge on the ACS Publications website at DOI: 10.1021/acscatal.5b01779.

Methods, additional spectroscopic and computational results and discussion, Figures S1–S4, and Tables S1 and S2 (PDF)

■ AUTHOR INFORMATION

Corresponding Author

*E-mail for N.M.M.: nmmarkovic@anl.gov.

Notes

The authors declare no competing financial interest.

■ ACKNOWLEDGMENTS

This work was supported as part of the Joint Center for Energy Storage Research (JCESR), an Energy Innovation Hub funded by the U.S. Department of Energy, Office of Science, Basic Energy Sciences. The submitted paper has been created by

UChicago Argonne, LLC, Operator of Argonne National Laboratory (“Argonne”). Argonne, a U.S. Department of Energy Office of Science laboratory, is operated under Contract no. DE-AC02-06CH11357. Work related to oxygen electrochemistry in alkaline solutions was supported by the U.S. Department of Energy, Basic Energy Science, Materials Science and Engineering Division.

■ REFERENCES

- (1) Tait, M. J.; Franks, F. *Nature* **1971**, *230*, 91–94.
- (2) Garrett, B. C. *Science* **2004**, *303*, 1146–1147.
- (3) Vöhringer-Martinez, E.; Hansmann, B.; Hernandez, H.; Francisco, J. S.; Troe, J.; Abel, B. *Science* **2007**, *315*, 497–501.
- (4) Marković, N. M.; Ross, P. N., Jr. *Surf. Sci. Rep.* **2002**, *45*, 117–229.
- (5) Magnussen, O. M. *Chem. Rev.* **2002**, *102*, 679–726.
- (6) Lipkowski, J. *Phys. Chem. Chem. Phys.* **2010**, *12*, 13874–13887.
- (7) Strmcnik, D.; Kodama, K.; van der Vliet, D.; Greeley, J.; Stamenkovic, V. R.; Marković, N. M. *Nat. Chem.* **2009**, *1*, 466–472.
- (8) Boda, D.; Fawcett, W. R.; Henderson, D.; Sokolowski, S. *J. Chem. Phys.* **2002**, *116*, 7170–7176.
- (9) Subbaraman, R.; Tripkovic, D.; Strmcnik, D.; Chang, K.-C.; Uchimura, M.; Paulikas, A. P.; Stamenkovic, V.; Markovic, N. M. *Science* **2011**, *334*, 1256–1260.
- (10) Danilovic, N.; Subbaraman, R.; Strmcnik, D.; Chang, K.-C.; Paulikas, A. P.; Stamenkovic, V. R.; Markovic, N. M. *Angew. Chem., Int. Ed.* **2012**, *51*, 12495–12498.
- (11) Strmcnik, D.; Uchimura, M.; Wang, C.; Subbaraman, R.; Danilovic, N.; van der Vliet, D.; Paulikas, A. P.; Stamenkovic, V. R.; Markovic, N. M. *Nat. Chem.* **2013**, *5*, 300–306.
- (12) Kinoshita, K. *Electrochemical Oxygen Technology*; Wiley: Hoboken, NJ, 1992.
- (13) Henderson, M. A. *Surf. Sci. Rep.* **2002**, *46*, 1–308.
- (14) Osawa, M.; Tushima, M.; Mogami, H.; Samjeské, G.; Yamakata, A. *J. Phys. Chem. C* **2008**, *112*, 4248–4256.
- (15) Ohta, N.; Nomura, K.; Yagi, I. *J. Phys. Chem. C* **2012**, *116*, 14390–14400.
- (16) Shao, M. H.; Adzic, R. R. *J. Phys. Chem. B* **2005**, *109*, 16563–16566.
- (17) Li, X.; Gewirth, A. A. *J. Am. Chem. Soc.* **2005**, *127*, 5252–5260.
- (18) Greeley, J.; Markovic, N. M. *Energy Environ. Sci.* **2012**, *5*, 9246–9256.
- (19) Stamenkovic, V.; Mun, B. S.; Mayrhofer, K. J. J.; Ross, P. N.; Markovic, N. M.; Rossmeisl, J.; Greeley, J.; Nørskov, J. K. *Angew. Chem., Int. Ed.* **2006**, *45*, 2897–2901.
- (20) Stamenkovic, V. R.; Fowler, B.; Mun, B. S.; Wang, G.; Ross, P. N.; Lucas, C. A.; Marković, N. M. *Science* **2007**, *315*, 493–497.
- (21) Adić, R. R.; Marković, N. M.; Vešović, V. B. *J. Electroanal. Chem. Interfacial Electrochem.* **1984**, *165*, 105–120.
- (22) Adžić, R. R.; Šrbac, S.; Anastasijević, N. *Mater. Chem. Phys.* **1989**, *22*, 349–375.
- (23) Zurilla, R. W.; Sen, R. K.; Yeager, E. *J. Electrochem. Soc.* **1978**, *125*, 1103–1109.
- (24) Sawyer, D. T.; Roberts, J. L. *J. Electroanal. Chem.* **1966**, *12*, 90–101.
- (25) Lu, Y.-C.; Gasteiger, H. A.; Shao-Horn, Y. *J. Am. Chem. Soc.* **2011**, *133*, 19048–19051.
- (26) Bruce, P. G.; Freunberger, S. A.; Hardwick, L. J.; Tarascon, J.-M. *Nat. Mater.* **2011**, *11*, 19–29.
- (27) Luntz, A. C.; McCloskey, B. D. *Chem. Rev.* **2014**, *114*, 11721–11750.
- (28) Kumar, N.; Radin, M. D.; Wood, B. C.; Ogitsu, T.; Siegel, D. J. *J. Phys. Chem. C* **2015**, *119*, 9050–9060.
- (29) Radin, M. D.; Rodriguez, J. F.; Tian, F.; Siegel, D. J. *J. Am. Chem. Soc.* **2012**, *134*, 1093–1103.
- (30) Schwenke, K. U.; Metzger, M.; Restle, T.; Piana, M.; Gasteiger, H. A. *J. Electrochem. Soc.* **2015**, *162*, A573–A584.
- (31) Sawyer, D. T.; Valentine, J. S. *Acc. Chem. Res.* **1981**, *14*, 393–400.
- (32) Laoire, C. O.; Mukerjee, S.; Abraham, K. M.; Plichta, E. J.; Hendrickson, M. A. *J. Phys. Chem. C* **2010**, *114*, 9178–9186.
- (33) Schwenke, K. U.; Meini, S.; Wu, X.; Gasteiger, H. A.; Piana, M. *Phys. Chem. Chem. Phys.* **2013**, *15*, 11830–11839.
- (34) Sawyer, D. T.; Chiericato, G.; Angelis, C. T.; Nanni, E. J.; Tsuchiya, T. *Anal. Chem.* **1982**, *54*, 1720–1724.
- (35) Koper, M. T. M. *Nanoscale* **2011**, *3*, 2054–2073.
- (36) Koper, M. T. M. In *Fuel Cell Catalysis; A surface science approach*; Wieckowski, A., Ed.; Wiley: Hoboken, NJ, 2009; pp i–xiii.
- (37) Janek, R. P.; Fawcett, W. R.; Ulman, A. *Langmuir* **1998**, *14*, 3011–3018.
- (38) Quaino, P.; Luque, N. B.; Nazmutdinov, R.; Santos, E.; Schmickler, W. *Angew. Chem., Int. Ed.* **2012**, *51*, 12997–13000.
- (39) Šrbac, S.; Adžić, R. R. *J. Electroanal. Chem.* **1996**, *403*, 169–181.
- (40) Hatzenbuhler, D. A.; Andrews, L. *J. Chem. Phys.* **1972**, *56*, 3398–3403.
- (41) Peng, Z.; Freunberger, S. A.; Hardwick, L. J.; Chen, Y.; Giordani, V.; Bardé, F.; Novák, P.; Graham, D.; Tarascon, J.-M.; Bruce, P. G. *Angew. Chem., Int. Ed.* **2011**, *50*, 6351–6355.
- (42) McCloskey, B. D.; Speidel, A.; Scheffler, R.; Miller, D. C.; Viswanathan, V.; Hummelshøj, J. S.; Nørskov, J. K.; Luntz, A. C. *J. Phys. Chem. Lett.* **2012**, *3*, 997–1001.
- (43) Adžić, R. R.; Tripković, A. V.; Marković, N. M. *J. Electroanal. Chem. Interfacial Electrochem.* **1980**, *114*, 37–51.
- (44) Adžić, R. In *Encyclopedia of Electrochemistry*; Wiley-VCH: Weinheim, Germany, 2007.
- (45) Das, U.; Lau, K. C.; Redfern, P. C.; Curtiss, L. A. *J. Phys. Chem. Lett.* **2014**, *5*, 813–819.